Ann. Geophys., 26, 3153–3158, 2008
www.ann-geophys.net/26/3153/2008/

Annales Geophysicae

Magnetic field disturbances in the sheath region of a super-sonic interplanetary magnetic cloud

E. Romashets[1], **M. Vandas**[2], **and S. Poedts**[3]

[1]Prairie View A& M University, Mail Stop 2250, P.O. Box 519, Prairie View TX 77446, USA
[2]Astronomical Institute, Academy of Sciences of the Czech Republic, Praha, Czech Republic
[3]Center for Plasma Astrophysics, K.U.Leuven, 200 B, 3001, Leuven, Belgium

Received: 12 October 2007 – Revised: 18 February 2008 – Accepted: 10 March 2008 – Published: 15 October 2008

Abstract. It is well-known that interplanetary magnetic clouds can cause strong geomagnetic storms due to the high magnetic field magnitude in their interior, especially if there is a large negative B_z component present. In addition, the magnetic disturbances around such objects can play an important role in their "geo-effectiveness". On the other hand, the magnetic and flow fields in the CME sheath region in front of the body and in the rear of the cloud are important for understanding both the dynamics and the evolution of the interplanetary cloud. The "eventual" aim of this work is to calculate the magnetic field in this CME sheath region in order to evaluate the possible geo-efficiency of the cloud in terms of the maximum $|B_z|$-component in this region. In this paper we assess the potential of this approach by introducing a model with a simplified geometry. We describe the magnetic field between the CME shock surface and the cloud's boundary by means of a vector potential. We also apply our model and present the magnetic field distribution in the CME sheath region in front of the body and in the rear of the cloud formed after the event of 20 November 2003.

Keywords. Interplanetary physics (Interplanetary shocks; Solar wind plasma) – Solar physics, astrophysics, and astronomy (Flares and mass ejections)

1 Introduction

Solar Coronal Mass Ejections (CMEs) play an important role in the triggering of magnetic storms on Earth. A lot of CMEs propagate in the interplanetary (IP) medium as magnetic clouds, usually at speeds that are higher than the speed of the ambient medium, i.e. the solar wind plasma. The faster IP magnetic clouds are accompanied by a CME shock and a CME sheath region around the central magnetic flux tube. There were many extensive studies of CMEs and magnetic clouds since the paper of Klein and Burlaga (1982). In the present paper we are only interested in fast CMEs because the interplanetary magnetic clouds related to the faster CMEs can cause strong geomagnetic storms, not only due to the magnetic field with high magnitude that is present in their interior, but also because of the CME sheath region around the cloud which also contains a magnetic field with a large negative B_z component. It was concluded by Zang et al. (2008), that the cloud's sheath area when it is present, can bring up to 29% additional energy into the magnetosphere. The magnetic field and the velocity field in the CME sheath region, which extends from the front to the rear part of the cloud, are both important for understanding the dynamics and the evolution of the interplanetary cloud. Moreover, the magnetic field in the magnetosheath area can contribute significantly to the "effectiveness" of the impact of the magnetic cloud on the Earth's magnetosphere.

There are various methods that can be applied to mathematically model the conditions in the CME sheath region around supersonic objects in general, and supersonic magnetic clouds in particular. However, most of these mathematical models can be used only within the so-called "rigid wall" approximation. The "rigid wall" approximation means that the boundary conditions are imposed on a fixed (a priori given) surface. The boundary position and the shape of the boundary are not calculated but set. A more accurate approach would give the surface position and shape from the balance of pressures on both sides of the surface as it was done, for example, in Romashets and Ivanov (1991). Some recent methods for the numerical calculation of flows past different bodies can be found in, e.g. Wu (1992); Lipatov et al. (2002); Omidi et al. (2002); Blanco-Cano et al. (2003); Raeder (2003). In case of magnetic clouds in the interplanetary space, however, such rigid wall conditions are not acceptable because the boundaries of these magnetic clouds are not fixed and their locations and sizes are changing in

Correspondence to: S. Poedts
(stefaan.poedts@wis.kuleuven.be)

Published by Copernicus Publications on behalf of the European Geosciences Union.

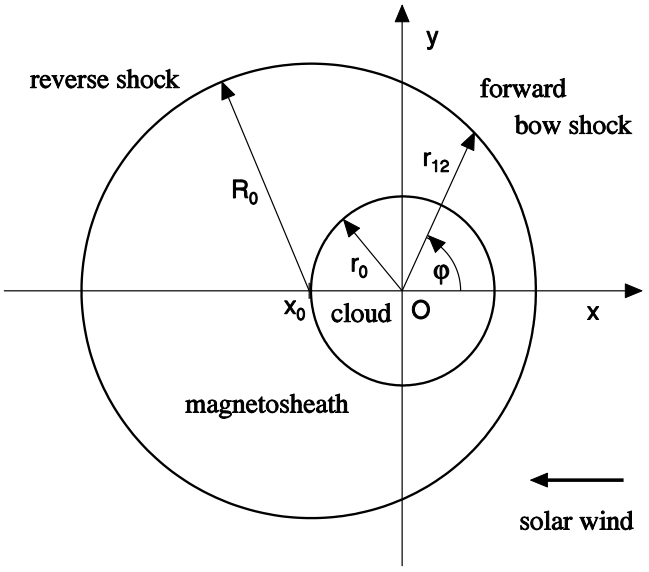

Fig. 1. Geometrical set-up of the considered problem (cut in the Z=0 plane). The particular case treated in Sect. 3 is displayed, with x_0=$-r_0$. But in general, x_0 can have an arbitrary value (limited by the geometry of the problem).

response to the varying parameters of the ambient plasma during the propagation of the cloud. Nevertheless, if these changes are smooth and they do not vary too fast, in comparison with the local Alfvén velocity, the so-called quasi-steady-state approximation can be applied. Romashets and Vandas (2005) used a similar approach as we use in the present paper. The only difference is that in Romashets and Vandas (2005) the magnetic field in the CME sheath region was given by a scalar potential. This means that there is no current present in the magnetosheath region. However, this is not compatible with the observations nor with the current physical insights regarding this problem. Another difficulty encountered in Romashets and Vandas (2005) is that, in some points on the modeled CME shock surface, the magnetic field does not increase but decrease in the shock. This magnetic field magnitude jump, resulting in magnetic field ratios B_2/B_1<1 (where B_1 indicates the magnetic field magnitude in the undisturbed solar wind plasma before the CME shock, and B_2 corresponds to the magnetic field magnitude at the magnetosheath side of the CME shock), was considered as a "small error" in that paper. In the present paper, we show how both these problems are solved at once by using a vector potential representation of the magnetic field in the CME sheath. As a matter of fact, the electric currents in the magnetosheath region are non-zero in our solutions, and the magnetic field magnitude jumps are all above unity on the CME shock.

In the next section, we present the new mathematical model and its solution. In Sect. 3, we present an application and we model the event of 29 November 2003. Finally, the conclusions are given in the last section in which we also address the limitations of the present model and possible future extensions.

2 Mathematical model and solution

We consider the two-dimensional set-up that is sketched in Fig. 1. We assume that the magnetic field in the entire volume between the cloud and the surrounding CME shock is described by the vector potential $\mathbf{A}(A_r, A_\varphi, A_Z)$, which is given by

$$A_r = 0, \tag{1}$$

$$A_\varphi = 0, \tag{2}$$

$$A_Z = B_0 r_0 \sum_{m=1}^{\infty} \frac{r^m - r_0^m}{r_{12}^m - r_0^m} \times (a_m \cos m\varphi + b_m \sin m\varphi), \tag{3}$$

in cylindrical coordinates r, φ, and Z. In this simple model, the boundary of the magnetic cloud is modeled as a cylinder with radius r_0 and with its central axis going through the point $O\equiv(0, 0)$, in Cartesian coordinates at the Z=0 plane. In other words, the cloud's axis coincides with the Z-axis (see Fig. 1, depicting a cross-section perpendicular to the Z-axis, i.e. the Z=0 surface). In the equation above, the constants a_m and b_m denote unit-less coefficients. The potential (1–3) ensures that the component of the external magnetic field normal to the cloud boundary (i.e. B_r), is zero. The A_Z component is constructed from this condition, in a way to ensure that there is enough flexibility at the CME shock surface, in order to be able to satisfy the required continuity of the normal component and an increase of magnetic field magnitude on it, i.e. $B_2/B1\geq1$. Among the large number of possible sets of functions that can satisfy these conditions, we have chosen this one, because the presence of terms like $\frac{r^m-r_0^m}{r_{12}^m-r_0^m}$ with correct coefficients, can ensure natural values of the magnetic field jump across the CME shock. The dependence on the angle φ is apparent, and is the same as in many other analytical solutions of similar problems. The CME shock surface is also treated as a cylinder but with radius R_0 and with its central axis going through the point $(x_0, 0)$ in the Z=0 plane, as illustrated in Fig. 1.

To satisfy the boundary conditions at the CME shock, we should require B_{1n}=B_{2n}, i.e. continuity of the normal component of the magnetic field. The unit vector normal to the CME shock in the point (x_{12}, y_{12}) is given by

$$n_x = \frac{x_{12} - x_0}{R_0}, \quad n_y = \frac{y_{12}}{R_0}, \tag{4}$$

in Cartesian coordinates, or, in cylindrical coordinates,

$$n_r = \frac{r_{12} - x_0 \cos\varphi}{R_0}, \quad n_\varphi = \frac{x_0 \sin\varphi}{R_0}. \tag{5}$$

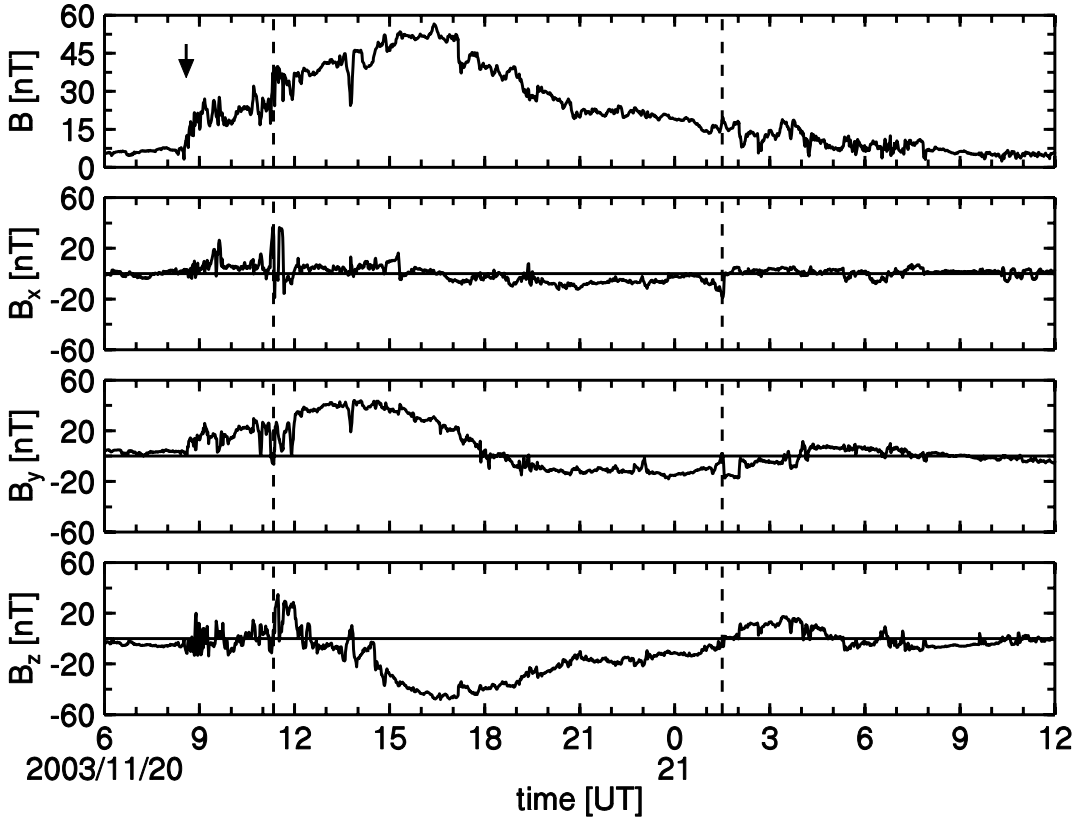

Fig. 2. Magnetic magnitude and components measured at 1 AU on 20 November 2003.

Here, $r_{12}(\varphi)=x_0\cos\varphi+\sqrt{R_0^2-x_0^2\sin^2\varphi}$ is the distance from the origin O to the point at the CME shock with coordinates $x_{12}=r_{12}\cos\varphi$ and $y_{12}=r_{12}\sin\varphi$. On the outer side of the CME shock we have

$$B_{1n} = B_{0x}n_x + B_{0y}n_y = \frac{B_{0x}(r_{12}\cos\varphi - x_0) + B_{0y}r_{12}\sin\varphi}{R_0}. \quad (6)$$

B_{0x} and B_{0y} are the components of the undisturbed interplanetary magnetic field (IMF) far from the magnetic cloud (constants). On the inner side, the normal component of the magnetic field is given by

$$\begin{aligned} B_{2n} &= B_r n_r + B_\varphi n_\varphi \\ &= \frac{B_0}{R_0}\sum_{m=1}^{\infty} m\,\{(r_{12}-x_0\cos\varphi) \\ &\quad\times\left[\left(\frac{r_{12}}{r_0}\right)^{m-1} - \left(\frac{r_0}{r_{12}}\right)^{m+1}\right] \\ &\quad\times(a_m\cos m\varphi + b_m\sin m\varphi) \\ &\quad + x_0\sin\varphi\left[\left(\frac{r_{12}}{r_0}\right)^{m-1} + \left(\frac{r_0}{r_{12}}\right)^{m+1}\right] \\ &\quad\times(-a_m\sin m\varphi + b_m\cos m\varphi)\}. \end{aligned} \quad (7)$$

Here, B_r and B_φ are the components of the magnetic field given by the vector potential (1–3),

$$\begin{aligned} B_r &= B_0\frac{r_0}{r}\sum_{m=1}^{\infty} m\frac{r^m - r_0^m}{r_{12}^m - r_0^m} \\ &\quad\times[-a_m\sin m\varphi + b_m\cos m\varphi \\ &\quad + \frac{r_{12}^{m-1}}{r_{12}^m - r_0^m}\left(x_0\sin\varphi + \frac{x_0^2\sin 2\varphi}{2\sqrt{R_0^2 - x_0^2\sin^2\varphi}}\right) \\ &\quad\times(a_m\cos m\varphi + b_m\sin m\varphi)], \end{aligned} \quad (8)$$

$$\begin{aligned} B_\varphi &= -B_0 r_0\sum_{m=1}^{\infty} m\,\frac{r^{m-1}}{r_{12}^m - r_0^m} \\ &\quad\times(a_m\cos m\varphi + b_m\sin m\varphi), \end{aligned} \quad (9)$$

expressed at $r=r_{12}$, and $B_0=\sqrt{B_{0x}^2+B_{0y}^2}$. As it has been mentioned before, the magnetic field is tangential to the cloud's surface, because $B_r=0$ at $r=r_0$ as can be seen from the form of the vector potential given by Eqs. (1–3).

By the selection of a limited set ($m\leq M$) of coefficients a_m and b_m in Eq. (7), one can achieve an approximate equity of Eqs. (6) and (7). The other condition, the condition of coplanarity, is automatically fulfilled since $B_Z\equiv 0$. It should be noted, however, that the approach for modeling the magnetic field in the magnetosheath of magnetic clouds, adopted

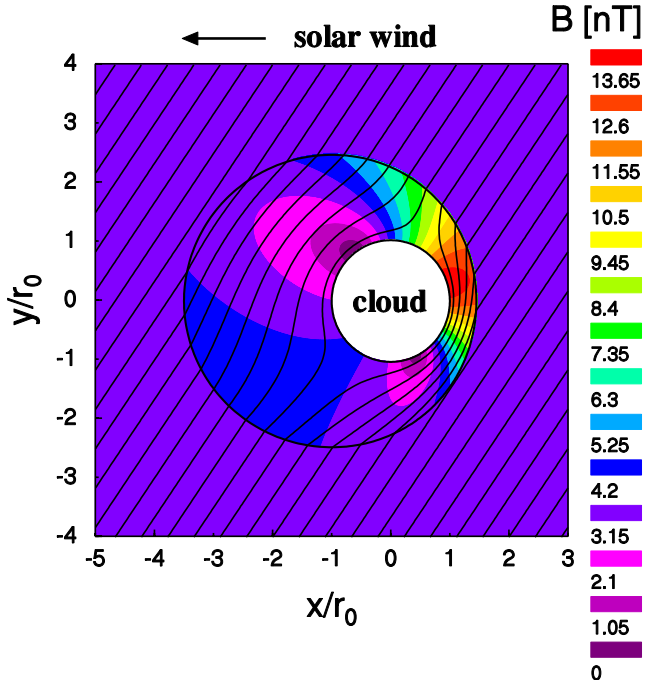

Fig. 3. Contours of |**B**| and field lines around the cloud.

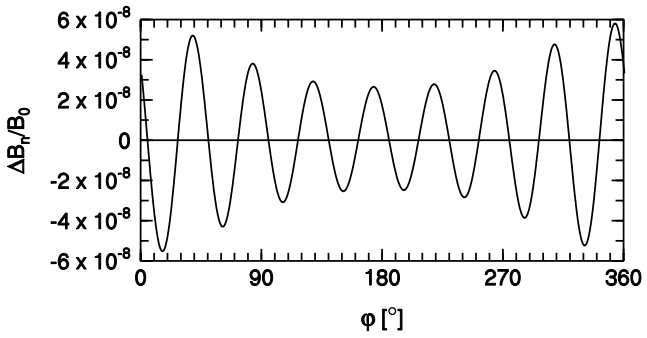

Fig. 4. Difference of B_n components at the CME shock.

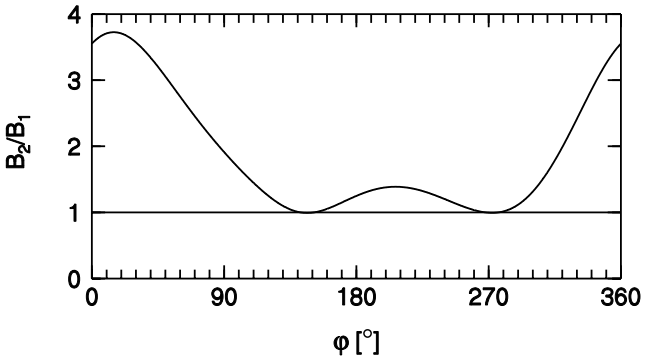

Fig. 5. Magnetic field magnitude jump at the CME shock.

in this paper, can also be applied when there is a B_Z component present. To meet the coplanarity condition, the determinant consisting of the components of the CME shock normal **n** and the magnetic fields in the CME sheath region $\mathbf{B}_i$ (inner) and upstream $\mathbf{B}_o$ (outer), just at the CME shock, must be zero. Using the fact that the normal magnetic field component is continuous at the CME shock, one arrives at the following expression for B_Z in the CME sheath:

$$B_{iZ}(r,\varphi) = B_{oZ}\,\frac{B^{12}_{i\varphi}(B^{12}_{i\varphi}-B^{12}_{o\varphi})+B^{12}_{ir}(B^{12}_{ir}-B^{12}_{or})}{B^{12}_{o\varphi}(B^{12}_{i\varphi}-B^{12}_{o\varphi})+B^{12}_{or}(B^{12}_{ir}-B^{12}_{or})}, \quad (10)$$

where $B^{12}_{i\varphi}=B_{i\varphi}(r_{12},\varphi)$, etc. For simplicity it is assumed that the component depends only on the coordinate φ. The solenoidality restriction requires that this component does not depend on Z. In fact, none of the model components depend on Z: this approximation is usually called a 2.5-D model.

3 Applications of the model

In order to compare our model with in-situ measurements, we searched for observations of magnetic clouds with a highly inclined axis, moving fast, and preceded by a well-developed CME shock wave. A low background B_z component was also desirable. There are few such candidates and, in fact, none of them fulfilled all these criteria completely.

Figure 2 shows WIND magnetic field observations (1 min averaged data from NSSDC) of the magnetic cloud of 20 November 2003. This cloud is listed in the WIND MFI (Magnetic Field Investigation) table of magnetic clouds (http://lepmfi.gsfc.nasa.gov/mfi/mag_cloud_S1.html) and also in the list by Huttunen et al. (2005). The former table gives a 76° inclination of the cloud, the latter 71°, so it is a highly inclined cloud. The vertical dashed lines show our estimate of magnetic cloud boundaries from the behaviour of the magnetic field components. They are not identical, but close to the identifications in the mentioned tables. The leading CME shock is marked by an arrow. The MFI Table yields 0.09 AU for the cloud radius and a nearly central crossing by the satellite. The duration of the leading CME sheath was about 3 h, so its thickness was about 0.04 AU (using averaged solar wind velocity of 600 km/s). In the model parameters it means that r_0=0.09 AU, R_0=2.5 r_0, and x_0=−1.0 r_0. The background magnetic field components were estimated from data to be B_{0x}=2 nT and B_{0y}=3 nT (in the GSE system).

This set of parameters resulted in the Figs. 3–5, so these are related to the event under study. We took a simple approach for this first comparison, viz. the magnetic cloud was regarded to be perpendicular to the ecliptic plane and the magnetic field components in this plane (B_x and B_y) were taken as relevant for the model; the B_z component was ignored (even though it is not negligible in comparison with the remaining components, but no more suitable example has

been found yet). In Fig. 6 we plotted the model magnetic field components (in GSE) and the magnitude of the magnetic field for the central crossing through the model cloud, i.e. along the x-axis. The first jump indicates the CME shock crossing and the entering into the CME sheath. The second small jump corresponds to the exit from the magnetosheath. The data gap is due to the passage of the proper cloud. The model shows that the magnetic field (B) magnitude is increasing in the magnetosheath behind the bow shock. The B_y component too is increasing in the magnetosheath, while the B_x component is diminishing. These features can also be qualitatively observed in the measured profiles (Fig. 2).

In Fig. 3, we display colored contours of the magnitude of the magnetic field together with magnetic field lines (in black).

On Fig. 4, we present the quantity $\Delta B_n/B_0$, i.e. the jump in the normal component of the magnetic field, at the CME shock as a function of φ. In the notation of the previous section, $\Delta B_n(\varphi)=B_{in}(r_{12},\varphi)-B_{on}(r_{12},\varphi)$. The field $\mathbf{B}_i$ is given by Eqs. (8–10) and $\mathbf{B}_o=\mathbf{B}_0$. One can see that the maximum of this ratio is a pretty negligible value, of the order of only 10^{-6}.

On Fig. 5, we present the CME shock jump $|\mathbf{B}_2|/|\mathbf{B}_1|$ as a function of φ. In the notation of the previous section, $\mathbf{B}_2(\varphi)=\mathbf{B}_i(r_{12},\varphi)$ and $\mathbf{B}_1(\varphi)=\mathbf{B}_o(r_{12},\varphi)=\mathbf{B}_0$. One can see that for all angles this jump is well above unity, as is required from observation data.

Hence, the results of the application of the simple model to this case with a uniform ambient field, displayed in Figs. 4–5, show a very good consistency with all the necessary conditions for this solution, viz. coplanarity, a jump of $|\mathbf{B}_2|/|\mathbf{B}_1|$ above unity everywhere on the CME shock, and the continuity of the normal component of the magnetic field at the CME shock ($\Delta B_n/B_0\approx 0$).

4 Conclusions

The distribution of the magnetic field is derived for both the forward and rear CME sheath regions around a supersonic cylindrical magnetic cloud in the solar wind. The model has also been applied to describe the magnetic field increase in the sheath area of a magnetic cloud observed on 20 November 2003. The model and measurements are qualitatively consistent for this specifically chosen event. Moreover, this result is qualitatively consistent with previous numerical calculations by Omidi et al. (2002) and Blanco-Cano et al. (2003). In these numerical calculations the maximum increase of the magnetic field magnitude B in the CME sheath is of the order of 3.5 times that of the ambient magnetic field. In the example considered in the present paper, this maximum increase of the magnetic field magnitude B in the magnetosheath is of the order of 4, as one can derive from Figs. 3.

In the present paper, we showed only one application where we compared magnetic cloud measurements with our model. We did so in order to demonstrate that the modeled magnetic field magnitude and orientation (i.e. the components) are at least qualitatively consistent with the measurements. In the near future we plan to interpret more events within the presented approach. However, to do so, it is necessary to first make our model more general. The next step is to construct a fully 3-D model, using Eq. (10). We plan to develop an analytical description of the sheath region of magnetic clouds with elliptical cross-sections. In addition, the formation of the CME sheath region will no longer be studied in a uniform outer magnetic field (as considered here), but in more complex magnetic fields, e.g. in a Parker spiral. Notice that our model describes the magnetic field in the CME sheath region to a first degree and on a macroscopic scale, which means that no wave activity can be considered or reproduced within this model. In reality, the CME sheath is a very perturbed region permeated by low frequency waves which can develop considerable amplitudes and change the properties of the region locally (Kataoka et al., 2005). The CME shock is composed of two regions, with quasi-parallel and quasi-perpendicular regimes, respectively, where waves can be generated and transmitted downstream. Moreover, due to existence of the foreshock, some waves are generated upstream so that the solar wind conditions prior to the CME shock are non-uniform.

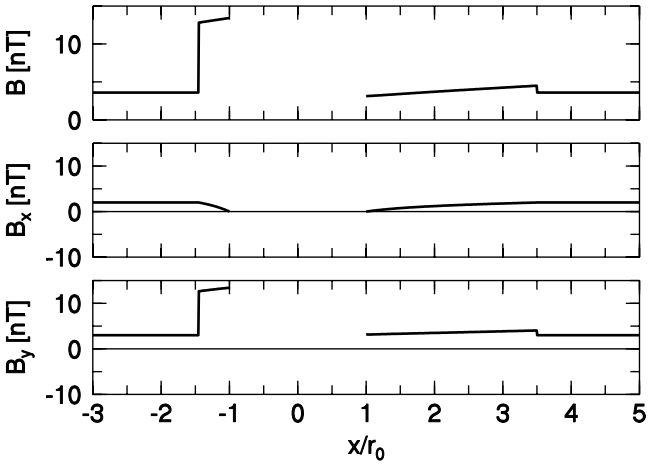

Fig. 6. Model magnetic field magnitude and components at 1 AU for 20 November 2003.

Our present model constructs only the magnetic field in the CME sheath, i.e. no plasma quantities are directly used or derived. This also is a serious simplification of the problem. Nevertheless, the plasma quantities are involved indirectly, e.g. through the stand-off distance of the CME shock from the cloud, which is one on the parameters of the model.

Acknowledgements. We acknowledge the use of data from NSSDC and the WIND MFI instrument in this work. The authors wish to express their gratitude to many colleagues for useful discussions. The work was supported by BELSPO, RFBR grant 06-05-64500,

EU/INTAS grant 03-51-6206, AV ČR project 1QS300120506, and GA ČR grant 205/06/0875. These results were obtained in the framework of the projects GOA 2004/01 (K. U. Leuven), G.0304.07 (FWO-Vlaanderen) and C90203 and C90196 (ESA Prodex 8).

Topical Editor R. Forsyth thanks two anonymous referees for their help in evaluating this paper.

References

Blanco-Cano, X., Omidi, N., and Russell, C. T.: Hybrid simulations of solar wind interaction with magnetized asteroids: Comparison with Galileo observations near Gaspra and Ida, J. Geophys. Res., 108, 1216, doi: 10.1029/2002JA009618, 2003.

Huttunen, K. E. J., Schwenn, R., Bothmer, V., and Koskinen, H. E. J.: Properties and geoeffectiveness of magnetic clouds in the rising, maximum and early declining phases of solar cycle 23, Ann. Geophys., 23, 625–641, 2005, http://www.ann-geophys.net/23/625/2005/.

Kataoka, R., Watari, S., Shimada, N., Shimazu, H., and Marubashi, K.: Downstream structures of interplanetary fast shocks associated with coronal mass ejections, Geophys. Res. Lett., 32, L12103, doi:10.1029/2005GL022777, 2005.

Klein, L. W. and Burlaga, L. F.: Magnetic clouds at 1 AU, J. Geophys. Res., 87, 613–624, 1982.

Lipatov, A. S., Motschman, U., and Bagdonat, T.: 3D hybrid simulations of the interaction of the solar wind with a weak comet, Planet. Space Sci., 50, 403–411, 2002.

Omidi, N., Blanco-Cano, X., Russell, C. T., Karimabadi, H., and Acuna, M.: Hybrid simulations of solar wind interaction with magnetized asteroids: General characteristics, J. Geophys. Res., 107, 1487, doi:10.1029/2002JA009441, 2002.

Raeder, J.: Global geospace modeling: Tutorial and review, in: Space Plasma Simulation, edited by: Buechner, J., pp. 212–246, 2003.

Romashets, E. and Ivanov, K. G.: Form of a magnetic cloud in the solar wind, Geomag. Aeron., 31, 470–472, 1991.

Romashets, E. and Vandas, M.: Field Structure Around a Super-Sonic Interplanetary Magnetic Clouds with Forward and Reverse Shocks, in: Proceedings of the Solar Wind 11/SOHO 16, edited by: Fleck, B., pp. 763–766, 2005.

Wu, C. C.: MHD flow past an obstacle: Large scale flow in the magnetosheath, Geophys. Res. Lett., 19, 87–90, 1992.

Zhang, J., Poomvises, W., and Richardson, I. G.: Sizes and relative geoeffectiveness of interplanetary coronal mass ejections and the preceding shock sheaths during intense storms in 1996–2005, Geophys. Res. Lett., 35, L02109, doi:10.1029/2007GL032045, 2008.